

VERSION 1
NOV 21, 2022

COMMENTS 0

Supplementary Material: An in silico approach to understanding the interaction between cardiovascular and pulmonary lymphatic dysfunction V.1

DOI

dx.doi.org/10.17504/protocols.io.kxygx9zmgw8j/v1

Kelly Burrowes¹

¹Auckland Bioengineering Institute, University of Auckland

WORKS FOR ME

1



Kelly Burrowes

ABSTRACT

The lung is extremely sensitive to interstitial fluid balance, yet the role of pulmonary lymphatics in lung fluid homeostasis and its interaction with cardiovascular pressures is poorly understood. In health, there is a fine balance between fluid extravasated from the pulmonary capillaries into the interstitium and the return of fluid to the circulation via the lymphatic vessels. This balance is maintained by an extremely interdependent system governed by pressures in the fluids (air and blood) and tissue (interstitium), lung motion during breathing, and the permeability of the tissues. Chronic elevation in left atrial pressure (LAP) due to left heart disease increases the capillary blood pressure. The consequent fluid accumulation in the delicate lung tissue increases its weight, decreases its compliance, and impairs gas exchange. This interdependent system is difficult, if not impossible, to study experimentally. Computational modelling provides a unique perspective to analyse fluid movement in the cardiopulmonary vasculature in health and disease. We have developed an initial *in-silico* model of pulmonary lymphatic function using an anatomically-derived structure to represent ventilation and perfusion, and underlying biophysical laws governing fluid transfer at the interstitium. This novel model was tested against increased LAP and non-cardiogenic effects (increased permeability). The model returned physiologically reasonable values for all applications, predicting pulmonary oedema when LAP reached 25 mmHg and with increased permeability.

DOI

dx.doi.org/10.17504/protocols.io.kxygx9zmgw8j/v1

PROTOCOL CITATION

Kelly Burrowes 2022. Supplementary Material: An in silico approach to understanding the interaction between cardiovascular and pulmonary lymphatic dysfunction. **protocols.io**
<https://dx.doi.org/10.17504/protocols.io.kxygx9zmgw8j/v1>
Version created by Kelly Burrowes

KEYWORDS

Pulmonary lymphatics, in silico models, cardio-pulmonary interdependence, pulmonary hypertension

LICENSE

This is an open access protocol distributed under the terms of the [Creative Commons Attribution License](https://creativecommons.org/licenses/by/4.0/), which permits unrestricted use, distribution, and reproduction in any medium, provided the original author and source are credited

CREATED

Nov 20, 2022

LAST MODIFIED

Nov 21, 2022

PROTOCOL INTEGER ID

73017

MATERIALS TEXT

Simulations performed on a regular desktop or laptop computer.

Lymphatic Model

1 *Estimation of interstitial hydrostatic pressure (P_{int})*

To represent this a sinusoidal function was used:

$$P_{int} = A \sin(B - C) + D$$

(S1)

A , the amplitude, is set to the difference between the maximum and minimum elastic recoil pressures for the acinus during a breath, as given by the ventilation model. This is representative of changes in thoracic pressure and is unique to each acinar unit. The change in period, B , is defined by the breathing frequency, where f_b is the breathing frequency in breaths per second. Multiplying B by time t will provide the exact value of B on the sine wave at that particular moment in time.

$$B = 2\pi f_b$$

(S2)

No horizontal shift is set, so C is equal to 0. Adding a vertical shift, D , enables the pressure to gradually fluctuate between -8 ($P_{min,int}$) and -1 mmHg ($P_{max,int}$) for the given amplitude. The vertical shift would be influenced by the interstitial saturation, and therefore can be scaled as a function of interstitial volume (V_{int}) over interstitial capacity (C_{int}). Furthermore, interstitial compliance is non-linear, having been observed to have low compliance at small volumes and high compliance at large volumes (1). An estimation of how these observations might manifest into a formula is through a polynomial function. To provide a unique relationship for each acinar unit the polynomial function is determined from the acinar unit amplitude as well as the interstitial pressure limits ($P_{min,int}$ and $P_{max,int}$).

$$D = (P_{min,int} - P_{max,int} + A) \left(\frac{V_{int}}{C_{int}} \right)^2 + \left(-2 (P_{min,int} - P_{max,int} + A) \right) \left(\frac{V_{int}}{C_{int}} \right) + \left(P_{min,int} + \frac{A}{4} \right)$$

(S3)

As interstitial volume approaches its maximal capacity the sinusoidal function (Equation A4) moves up the y-axis, indicating greater pressures within the interstitium. Combined, the overall equation for interstitial pressure becomes:

$$P_{int} = A \sin((2\pi t f_b) - 0) + (P_{min,int} - P_{max,int} + A) \left(\frac{V_{int}}{C_{int}} \right)^2 + \left(-2 (P_{min,int} - P_{max,int} + A) \right) \left(\frac{V_{int}}{C_{int}} \right) + \left(P_{min,int} + \frac{A}{2} \right)$$

(S4)

This relationship is plotted in Figure A1.

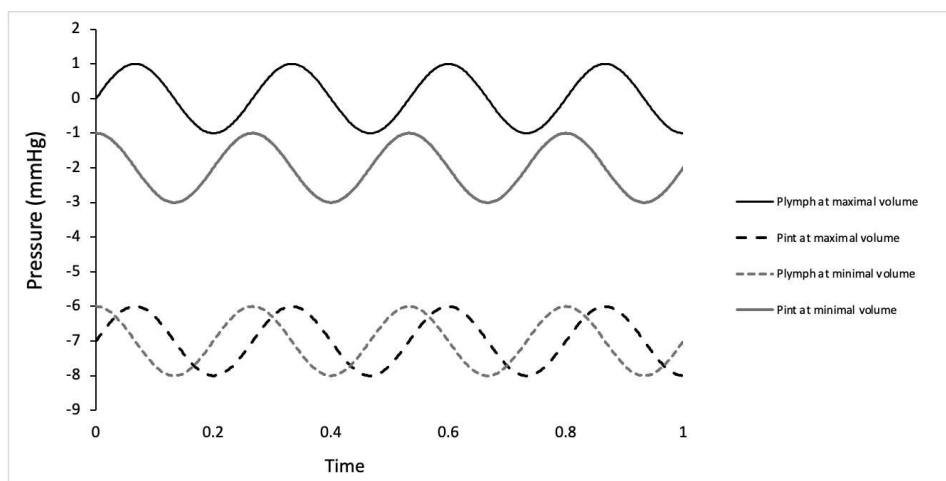


Figure S1: Plot of pressure versus time demonstrating the sinusoidal relationships for the hydrostatic pressure in the interstitial space (Pint, Equation S4) and hydrostatic pressure in the lymph space (Plymph, Equation S6).

2 **Lymphatic hydraulic conductivity**

Lymphatic hydraulic conductivity, L_{lymph} is estimated using the following equation:

$$L_{p_{lymph}} = L_{p_{cap}} \alpha_1 \left(\frac{V_{int}}{C_{int}} \right)^5 + \alpha_2 \left(\frac{V_{int}}{C_{int}} \right)^4 + \alpha_3 \left(\frac{V_{int}}{C_{int}} \right)^3 + \alpha_4 \left(\frac{V_{int}}{C_{int}} \right)^2 + \alpha_5 \left(\frac{V_{int}}{C_{int}} \right) + \alpha_6$$

(S5)

Coefficients α_{1-6} were approximated using a trial and error method using a single, representative acinar unit (selected from the middle of the right lung) to meet the following conditions:

- Alveolar flooding occurs when left atrial pressure is 25 mmHg.
- An increase in interstitial saturation without flooding when left atrial pressure is 20 mmHg.
- Resting steady-state interstitial saturation is ~48%.
- A 50% increase or decrease in baseline saturation would return to resting steady-state values.

This provided the coefficients displayed below in Table S1.

A	B
Coefficient	Value
α_1	846
α_2	-2417
α_3	2389
α_4	-922
α_5	126
α_6	0

Table S1: Coefficients used for calculating lymphatic conductivity (Equation S5)

In reality, there is a baseline rate of conductivity that is only increased when interstitial volume reaches the threshold at which anchoring filaments begin to open initial lymphatic pores. Therefore, when interstitial saturation is 30% or less, $L_{p_{lymph}}$ is held constant at $6.5e^{-8} \text{ ml s}^{-1} \text{ mmHg}^{-1}$, or 1.48 times more than capillary conductivity (Figure S2).

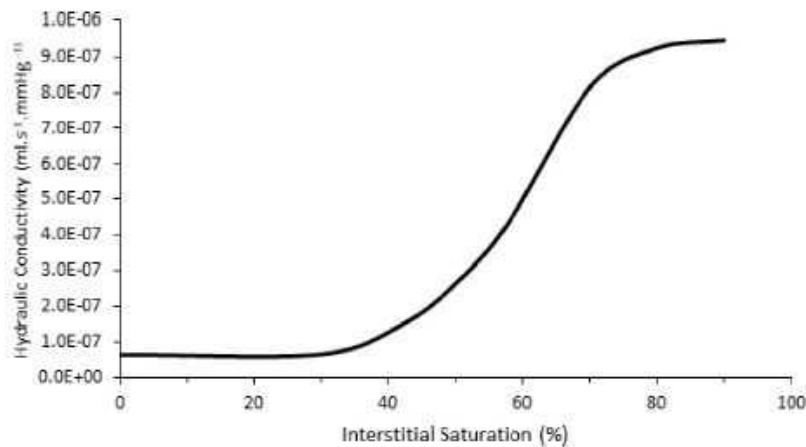


Figure S2: Relationship between interstitial saturation and hydraulic conductivity.

3 **Estimation of lymphatic hydrostatic pressure**

The hydrostatic pressure gradient of the lymphatics was approximated using the following equation, similar to that described above in Equation S4:

$$P_{hyd,lymph} = \frac{A}{2} \sin\left((2\pi t f_b) + \frac{\pi}{2}\right) + (P_{max,lymph} - P_{min,lymph} - A) \left(\frac{v_{int}}{C_{int}}\right)^2 + \left(P_{min,int} + \frac{A}{2}\right),$$

(S6)

where interstitial volumes and capacities are assumed to represent the likely saturation of the lymphatics in equilibrium, in the absence of anatomical information of the initial lymphatics. The equation also includes the C value from Equation A5 that represents the horizontal offset, $\pi/2$, which is a quarter-cycle offset. The offset enables the cyclical fluctuations in interstitial and initial lymphatic pressure to overlap, simulating the transient pressure differences between the two compartments that are hypothesised to exist (2-4). This relationship is plotted in Figure S1.

Perfusion Model

- 4 The perfusion module simulates pulmonary blood supply within the pulmonary vasculature. The arterial tree is comprised of asymmetrically bifurcating elements that represent the arterial vasculature, which supplies $\sim 32,768$ (2^{15}) vessels that feed the acinar units at the level of the terminal bronchioles in the airway tree. Within the acinar unit model, these arterioles continue to bifurcate symmetrically through 9 generations of capillaries, each connected across the alveoli to a corresponding venule creating a ladder-like structure (5). Each capillary is treated as a 'sheet' that transverses multiple alveoli, with each sheet having a specific model-calculated flow rate, blood pressure and surface area, unique to the capillary generation of that acinar unit (6).

These values are dependent on the resistance of each unit's supplying arterial pathway, the amount of expansion each unit undergoes with breathing, and the gravitational influence to establish a hydrostatic pressure gradient (7) (Equation S7). Once the blood has flowed through the capillaries, the venous network continues to transport the fluid out of the lung using a venous tree that mirrors the structure of the arterial tree. A steady flow is simulated, which can be altered by changing the boundary conditions (inlet pressure/flow and the outlet pressure/flow).

$$\Delta P = \frac{128\mu L}{\pi D^4} Q + \rho g \cos\theta L$$

(S7)

where μ is blood viscosity, L is the vessel length, D is the vessel diameter, Q is the blood flow rate, ρ is the density of blood in the vessel, g is gravitational acceleration 9.81 m/s and θ is the angle of the vessel with respect to gravitational direction. This equation, alongside conservation of mass, is solved through the full network and provides values of capillary hydrostatic pressure ($P_{hyd,cap}$), capillary blood volume (V_{cap}) and the flow rate (Q_{cap}) – to calculate blood transit time as $t_{transit}=V_{cap}/Q_{cap}$ used in the lymphatic model.

In addition to altering capillary pressure, modifying boundary conditions also changes the transit time of blood through a capillary bed and the capillary surface area. Whole lung capillary surface area at total lung capacity (TLC) is estimated to be 73 m²(5, 8), which can be divided by the number of acinar units to provide S_{cap} the surface area for an individual acinus at TLC (S_{TLC}). However, if the alveolus is not fully inflated S_{cap} needs to be scaled accordingly, based on lung compliance (C) and transpulmonary pressure (P_{tp}), as described by Clark et al. (5) (Equation S8). Additionally, if alveolar air pressure (P_{alv}) is greater than venous pressure (P_{bv}) parts of the alveolar sheet can collapse - this is the so called 'zone 2' flow region. In this zone of flow, the available capillary surface area ($S_{cap,zone2}$) is reduced by the factor described in Equation S9 as defined by Fung and Yen (9) (Equation S9), which is integrated with Equation S8 to provide the capillary surface area to be used within the lymphatic model.

$$S_{cap} = S_{TLC} \left(\frac{V}{V_{TLC}} \right)^{2/3} = S_{TLC} (1 - 0.8e^{-CP_{tp}})^{2/3}$$

(S8)

$$S_{cap,zone2} = S_{cap} \left(1 - F + F e^{\left[-\frac{P_{bv} - P_{alv}^2}{2\sigma^2} \right]} \right),$$

(S9)

where F is the maximum fraction of alveolar area that can be collapsed and σ is a constant that determines the extent of capillary collapse for a change in P_{bv} .

Ventilation Model

- 5 Elastic recoil pressure was calculated for each acinus using a relationship derived by Swan et al. (10), as shown in Eq. A4. Here, P_e is approximated from a 3D strain energy density relationship by assuming that each acinus expands isotropically. λ is the isotopic strain (Eq. 4) calculated from the current acinus volume (V) and its undeformed volume (V_0).

$$P_e = \frac{\xi e^\gamma}{2\lambda} (3a + b)(\lambda^2 - 1),$$

(S10)

where γ is equal to

$$\frac{3}{4} (3a + b)(\lambda^2 - 1)^2$$

and λ is the isotropic stretch from the undeformed reference volume (V_0), calculated as

$$\lambda = \sqrt[3]{V/V_0}.$$

Estimated strain energy density function values are ξ , 2500 Pa (11); a , 0.433 (12); b , -0.611 (12)). Maximum and minimum elastic recoil pressure values are used as a surrogate of the change in pressure within the thoracic cavity within the lymphatics model (Figure 1).

References

1. **Taylor A, and Parker J.** Pulmonary Interstitial Spaces and Lymphatics. *Comprehensive Physiology* 2011.
2. **Svendsen Ø, Reed R, and Wiig H.** The Interstitium and Lymphatics have an Important Role in Edema Generation during Sepsis. In: *Annual Update in Intensive Care and Emergency Medicine 2011*, edited by Vincent J. Berlin: Springer, 2011.
3. **Sabine A, Saygili Demir C, and Petrova TV.** Endothelial Cell Responses to Biomechanical Forces in Lymphatic Vessels. *Antioxidants & redox signaling* 25: 451-465, 2016.
4. **Zawieja D.** Contractile Physiology of Lymphatics. *Lymphatic Research and Biology* 7: 87-96, 2009.
5. **Clark AR, Burrowes KS, and Tawhai MH.** Contribution of serial and parallel micro-perfusion to spatial variability in pulmonary inter- and intra-acinar blood flow. *Journal of Applied Physiology* 108: 1116-1126, 2010.
6. **Fung YC, and Sobin SS.** Theory of sheet flow in lung alveoli. *Journal of Applied Physiology* 26: 472-488, 1969.
7. **Clark AR, Tawhai MH, Hoffman EA, and Burrowes KS.** The interdependent contributions of gravitational and structural features to perfusion distribution in a multiscale model of the pulmonary circulation. *Journal of Applied Physiology* 110: 943-955, 2011.
8. **Gehr P, Bachofen M, and Weibel ER.** The normal human lung - Ultrastructure and morphometric estimation of diffusion capacity. *Respiratory Physiology and Neurobiology* 32: 121-140, 1978.
9. **Fung YC, and Yen RT.** A new theory of pulmonary blood flow in zone 2 condition. *Journal of Applied Physiology* 60: 1638-1650, 1986.
10. **Swan AJ, Clark AR, and Tawhai MH.** A computational model of the topographic distribution of ventilation in healthy human lungs. *J Theor Biol* 300: 222-231, 2012.
11. **Tawhai MH, Nash MP, Lin CL, and Hoffman EA.** Supine and prone differences in regional lung density and pleural pressure gradients in the human lung with constant shape. *J Appl Physiol* 107: 912-920, 2009.
12. **Kowalczyk P, and Kleiber M.** Modelling and numerical analysis of stresses and strains in the human lung including tissue-gas interaction. *European Journal of Mechanics - A-Solids* 13.3: 367-393, 1994.